Multiscale Network Models (D1.4 - SGA3)

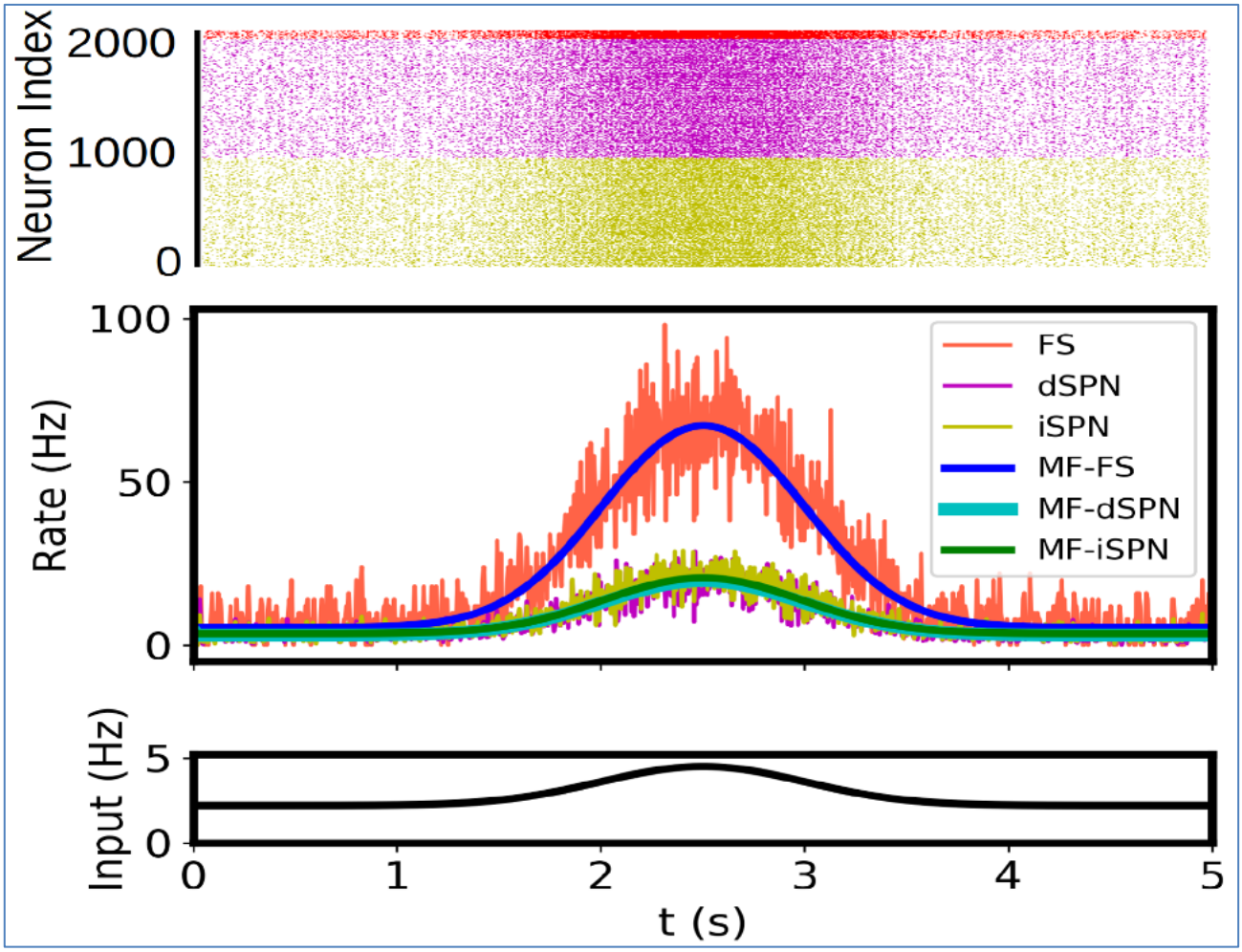

Figure 1: Construction and validation of a mean-field model of basal ganglia circuits.

This model is derived from microcircuits and is compatible with implementation in The Virtual Brain to perform whole-brain simulations, including basal ganglia (collaboration between Partners KI and CNRS).

.

Project Number:	945539	Project Title:	HBP SGA3

Document Title:	Multiscale Network Models
Document Filename:	D1.4 (D10) SGA3 M36 SUBMIT 230405
Deliverable Number:	SGA3 D1.4 (D10)
Deliverable Type:	Demonstrator
Dissemination Level:	PU = Public
Planned Delivery Date:	SGA3 M36 / 31 Mar 2023
Actual Delivery Date:	SGA3 M37 / 5 Apr 2023
Author(s):	Alain DESTEXHE, CNRS (P10) Federico TESLER, CNRS (P10)
Compiled by:	Alain DESTEXHE, CNRS (P10)
Contributor(s):	Roberta LORENZI, UNIPV (P70), contributed to Sections 2.2.2 and 2.2.4 Claudia CASELLATO, UNIPV (P70), contributed to Section 2.2.4 Alice GEMINIANI, UNIPV (P70), contributed to Section 2.2.4 Alexander KOZLOV, KTH (P39), contributed to Section 2.2.3 Adam PONZI, CNR (P12), contributed to Section 2.2.2 Jan FOUSEK, AMU (P78), contributed to Section 2.3 Gorka ZAMORA-LOPEZ, UPF (P77), contributed to Section 2.4 Idan SEGEV, HUJI (P60), contributed to Section 2.1.1 Michele MIGLIORE, CNR (P12), contributed to Section 2.1.2 Sten GRILLNER, KI (P37), contributed to Section 2.1.3 Jeanette HELLGREN, KTH (P39), contributed to Section 2.4 Egidio D'ANGELO, UNIPV (P70), contributed to Sections 2.1.4 and 2.2.4 Gustavo DECO, UPF (P77), contributed to Section 2.4 Viktor JIRSA, AMU (P78), contributed to Section 2.3 Federico TESLER, CNRS (P10), contributed to Sections 2.2.2 and 2.2.3 Alain DESTEXHE, CNRS (P10), contributed to Sections 1, 2.2.1 and 3
WP QC Review:	Giovanna RAMOS QUEDA, AMU (P78), Pilar F. ROMERO, UPM (P68)
WP Leader / Deputy Leader Sign Off:	Viktor Jirsa, AMU (P78)
T7.4 QC Review:	Martin TELEFONT, EBRAINS (P1)
Description in GA:	Demonstrators will be available in EBRAINS featuring a multiscale data-driven network model (microcircuit models for cortex, cerebellum, hippocampus, basal ganglia) using Neuron and NEST, and mean field models integrating the specifics of each brain region; model will be integrated in WP1 brain reference framework, and will be informed and validated against empirical data sets, including parameter maps for neuroreceptors, molecular regulators and their complexes with cellular partners.
Abstract:	This Deliverable covers models that will be available in EBRAINS, featuring a multiscale data-driven network model (microcircuit models for cortex, cerebellum, hippocampus and basal ganglia) using Neuron and NEST, and mean field models integrating the specifics of each brain region. The models will be integrated in the WP1 brain reference framework, and will be informed and validated against empirical data sets, including parameter maps for neuroreceptors, molecular regulators and their complexes with cellular partners.
Keywords:	Microcircuit models, mean-field models, whole-brain models
Target Users/Readers:	Computational neuroscience community, neuroimaging community, neuroinformaticians, neuroscientific community, neuroscientists, platform users, researchers, scientific community, students

Table of Contents

Table of Figures

1. Introduction

In this Deliverable, we describe the design of microcircuit models of different human brain regions: cerebral cortex, hippocampus, basal ganglia and cerebellum. These models describe activity at microscales (local circuit), up to mesoscale (typically millimetres). In some cases, these microcircuit models can comprise morphologically detailed models of single cells, typically simulated using the NEURON simulator. Alternatively, microcircuit models can be made of point neurons, either Hodgkin-Huxley (HH) or different types of integrate-and-fire (IF) models. Such point neuron model networks are typically simulated with simulators such as BRIAN or NEST.

To reach larger scales than microcircuit models, we developed models aimed at investigating populations of neurons (mesoscale to macroscale). Here, our approach was to design mean-field models, in which we started from the spiking model level and construct a mean field (bottom-up) to yield a population model. Typically, such mean-field models describe the activity of excitatory and inhibitory neuron populations with a compact set of equations. Such mean fields can then be connected into networks of mean fields, to describe the activity of neural tissue at scales from millimetres to centimetres. Ultimately, the mean fields can be integrated in specific simulation tools, such as The Virtual Brain (TVB), simulating the whole cortex or whole-brain.

In this Deliverable, we describe this integration. This work is related to the multiscale integration goal of the HBP, as well as to SGA3 Showcase 3.

2. Description of the models in the Deliverable

2.1 Microcircuit models

2.1.1 Microcircuit models of cerebral cortex (HUJI)

The Segev group at the Hebrew University of Jerusalem, in collaboration with the C. deKoch team at the Free University in Amsterdam, constructed models of connected pairs of L2/3 cortical pyramidal cells. Synaptic transmission between these pyramidal neurons was based on neurosurgically-resected human middle temporal gyrus (MTG, Brodmann area 21). Local connectivity is comparable to mouse Layer 2/3 connections in the temporal association area, but synaptic connections in human are 3-fold stronger and more reliable (0% vs. 25% failure rates, respectively). We developed a theoretical approach to quantify properties of spinous synapses showing that synaptic conductance and voltage change in human dendritic spines are 3-4 fold larger compared to mouse, leading to significant NMDA receptor activation in human unitary connections. This model prediction was validated experimentally by showing that NMDA receptor activation increases the amplitude and prolongs decay of unitary excitatory postsynaptic potentials in human but not in mouse connections. See details in Hunt *et al*. 2022, P3873.

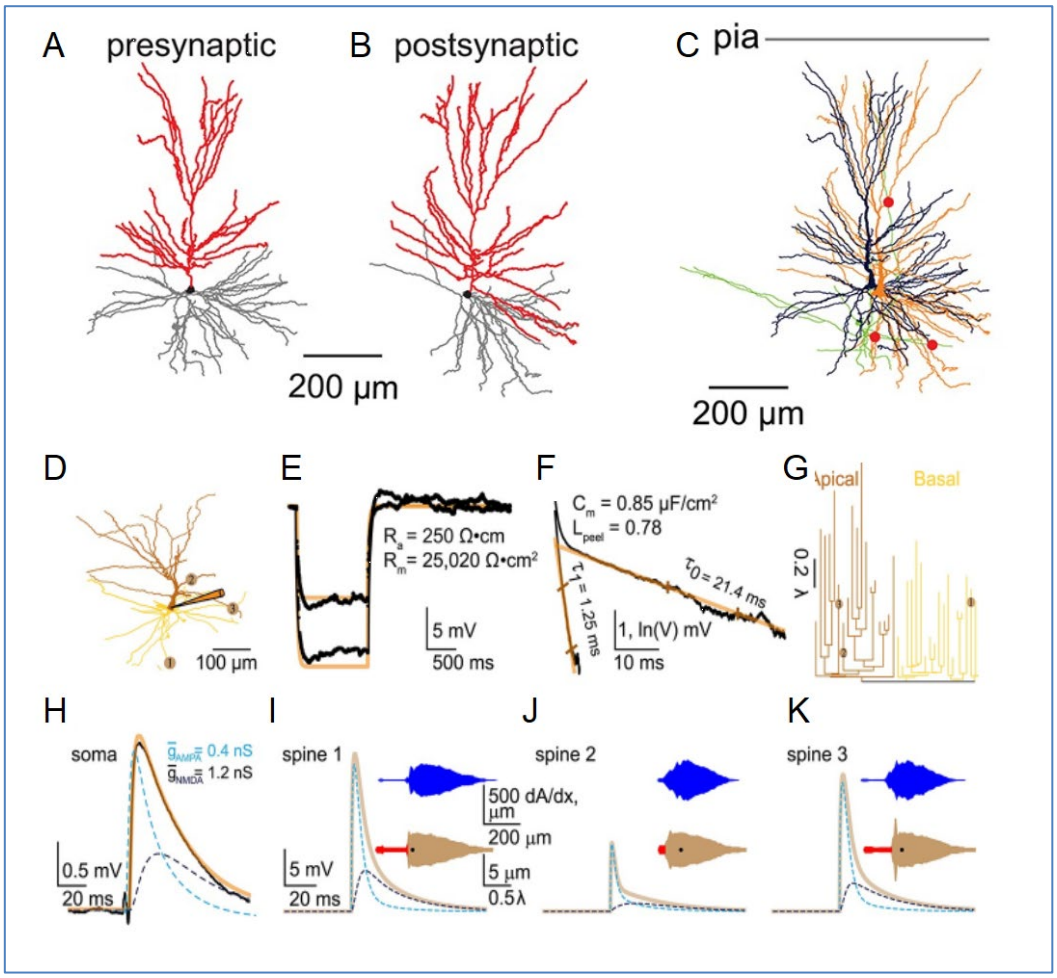

Figure 2: Human cerebral cortex model

A, B: Pre-and post-synaptic Human L2/3 cortical pyramidal neurons. C: Location of putative synapses between the cells shown in A and B. D: Modelled human L2/L3 neuron with dendritic locations of 3 synaptic contacts (numbered circles) originating from a single presynaptic L2/L3 neuron. Apical and basal trees are marked in dark and light orange respectively, schematic electrode at soma is also shown. E: Somatic voltage response (black traces) for the neuron shown in a) to 2 steady hyperpolarizing current inputs (here, −62 and −108 pA) and the corresponding model fit (brown traces) with respective model values for R_a and R_m. F: "Peeling" of somatic voltage transient in response to a brief (2 ms) hyperpolarizing step current (not shown) in the neuron shown in a). τ_0, extracted from this peeling, together with R_m as in b), are used to calculate C_m, whereas P_{eel} value is computed from $\tau_1$and τ_0 (see Methods). G: Electrotonic dendrograms of the neuron shown in a, with locations of the three synaptic contacts. H: Experimental somatic EPSP (black trace) in response to a presynaptic spike with model fit superimposed (light brown). Synapses were activated on modelled dendritic spines. AMPA- and NMDA- components of the modelled EPSP are also shown (dashed lines) with their respective maximal conductances value (at each synaptic contact). The NMDA-component is calculated by subtracting the AMPA component of the EPSP from the AMPA- plus NMDA-based EPSP. I, J, K: Computed EPSPs and respective AMPA- and NMDA-components at the spine head membrane located at the three synaptic sites shown in a). The upper (blue) and lower (red/brown) insets show, respectively, the spatial distribution of the neuron's membrane area a) as a function of the physical distance, x, from the spine and the "equivalent cable" as seen from the spine perspective (spine is located at left end of these insets, soma location is marked by the black dot, see Methods). Observing the "equivalent cable" insets, the electrotonic decoupling of spine #1 and #3 from the impedance load due to the respective red cable (at the left of inset) results in relatively large EPSPs at these spines, whereas the large impedance load that is adjacent to spine #2 results in a relatively small EPSP at this spine.

2.1.2 *Microcircuit models of hippocampus (CNR)*

Partner CNR reported the availability of a preliminary full-scale NEST model of the human hippocampal CA1 region at cellular level (Figure 3), now is available on the EBRAINS KG. A preliminary full-scale NEST model of the human hippocampal CA1 region at cellular level is available on the EBRAINS KG at this link https://search.kg.ebrains.eu/instances/7fb22b04-5fe1-4f18-b0d0-dc1386f90f83.

A paper on its implementation is in press (Gandolfi *et al.*, 2023, in press). The model is based on data obtained from the analysis of histological human brain images, which are publicly available from the BigBrain Jülich repository[1]. A custom-made computational algorithm has been developed to extract the positions of neuronal somata from the images. A second custom-made algorithm has been developed to connect neurons following morpho-anatomical landmarks. The full matrix of neuronal positioning, together with the indices of connected neurons, is provided as a connection matrix, in order to be used for large-scale simulations with single point neurons implemented in NEST.

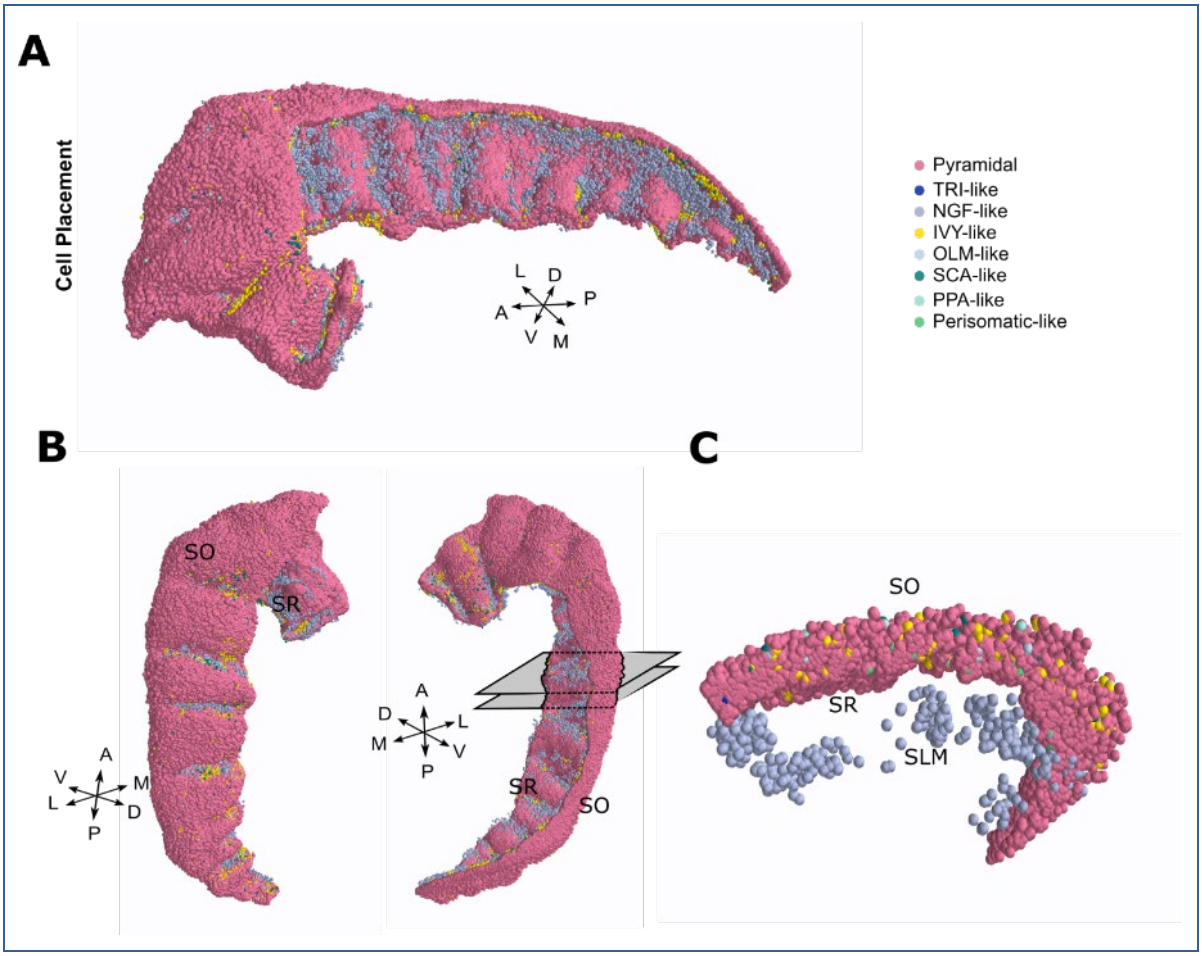

Figure 3: Human hippocampus model

A. 3D positioning of the excitatory (Pyramidal, pink) and inhibitory neurons. Interneurons are divided into 7 classes, according to positioning and morphological features. B. Reoriented 3D neuronal positioning shown in A to highlight interneurons distribution. C. 2mm transversal slice of 3D positioning obtained from sectioning CA1 between the two grey shaded planes shown in B, right. Note the NGF-like neurons (grey spots) in the lower part corresponding to Stratum Radiatum (SR), Stratum Lacunosum-Molecularis (SLM), and Ivy-like neurons (yellow spots) scattered within the Pyramidal layer (SP).

2.1.3 Microcircuit models of basal ganglia (KI)

The computational model of the basal ganglia we use here for the action selection is based on detailed multicompartmental simulations (Hjorth *et al.*, 2020, P2489 and Frost Nylén *et al.*, 2021, P2674) that have then been reduced to NEST. It follows the classical concept of the direct and indirect pathways throughout the basal ganglia (Figure 4), which compete for the activity of the output channel in substantia nigra pars reticulata (SNr) or globus pallidus interna (GPi). Tonic activity of the GABA-ergic output nucleus inhibits the downstream action-specific command centre and can be facilitated to prevent corresponding action or suppressed to release it through disinhibition. The dorsal striatum makes the major input stage of the basal ganglia and lays down the two main

[1] BigBrain: https://search.kg.ebrains.eu/instances/af8d3519-9561-4060-8da9-2de1bb966a81

pathways which originate in the pools of striato-nigral projection neurons (dSPN) and striato-pallidal projection neurons (iSPN), both inhibited by fast-spiking interneurons (FS). Cortical command to the dSPN pool which inhibits activity in SNr and releases the action is interpreted as “Go” signal, while the command applied to iSPN pool which indirectly increases the output activity in SNr, acting via inhibitory globus pallidus externa (GPe) and excitatory subthalamic nucleus (STN), makes a “No-Go” signal. Action selection within this concept is understood as a result of the competition between the “Go” and “No-Go” signals, which originates in the striatum.

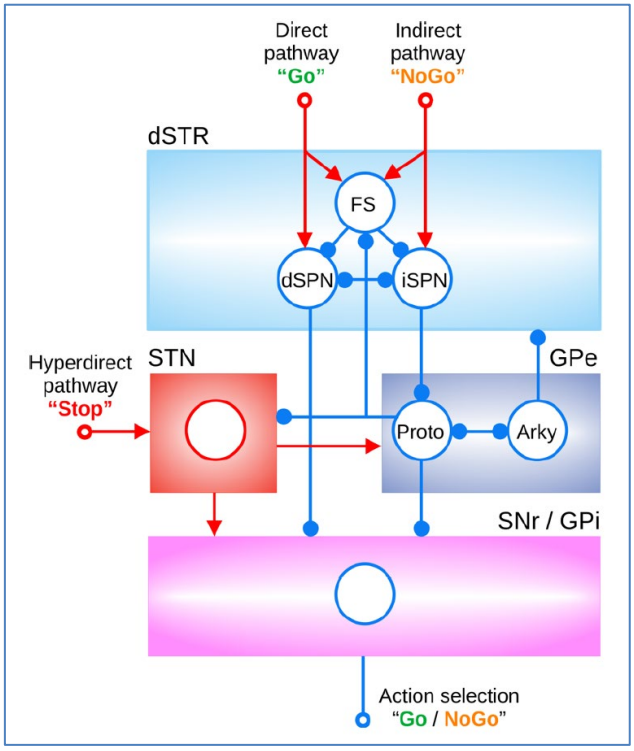

Figure 4: Conceptual model of the basal ganglia for action selection used for the NEST model

Excitatory and inhibitory projections are shown in red and blue, respectively.

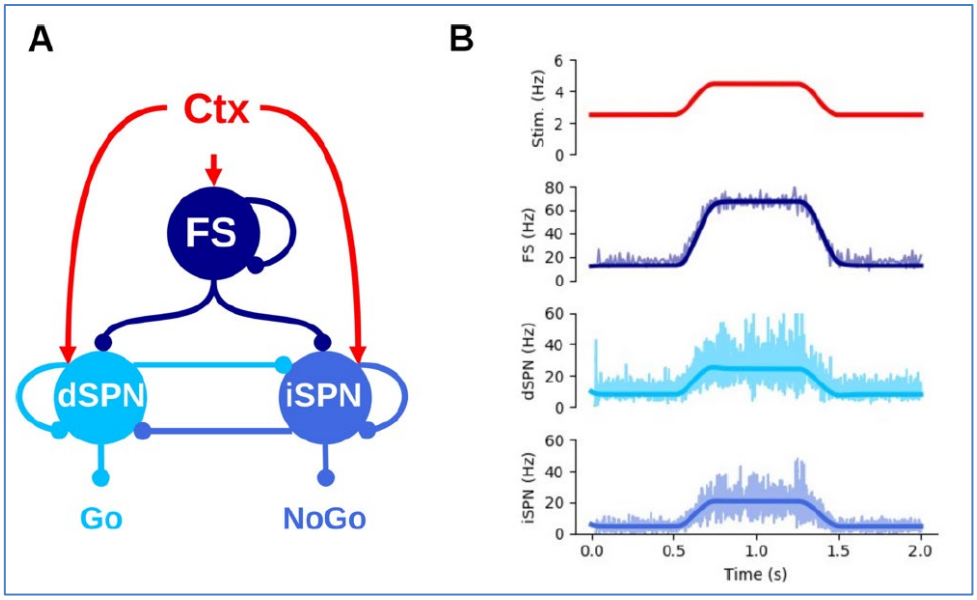

Figure 5: Mean-field model of the dorsal striatum based on simulation in NEST

A: Striatal circuit. Inhibitory connections are marked with dots, excitatory inputs are shown with arrows. Population of fast-spiking interneurons (FS) provides feed-forward inhibition to the interconnected pools of the direct- and indirect-pathway striatal projection neurons (dSPN, iSPN). B: The solid lines represent the mean field, which is based on the NEST simulation represented as the jitter in the blue traces, colour-coded for FS, dSPN and iSPN as in the scheme in A. The cortical command is in red. Instantaneous firing rates in the spiking network model are shown with semi-transparent jittered lines. Overlaid solid lines correspond to the mean-field model.

Dynamics of the dorsal striatum are simulated using spiking neural networks (NEST), as well as the non-spiking mean-field mathematical approximation of the underlying activity. The mean field model is also represented in the next section (Figure 12 and Figure 13). The circuitry of the corresponding simulations is shown in Figure 5A. The cortical command (Ctx, in red) is simulated as a Poissonian excitatory synaptic input in the network simulations, or a continuous firing rate signal in the mean-field approximation (see Figure 5B, red line). Populations of FS, dSPN and iSPN cells are modelled using adaptive exponential integrate and fire neurons (AdEx) and the connectivity is set to the values obtained in biologically detailed large-scale simulations (Hjorth *et al.*, 2020, P2489).

2.1.4 Microcircuit models of cerebellum (UNIPV)

Partner UNIPV reports the publication of the first full microcircuit model of the cerebellar cortex (De Schepper *et al.*, 2022, P3729), along with the presentation of the modelling component workflow "Brain Scaffold Builder"[2], which is now made available through EBRAINS.

The model of the cerebellum was generated accounting for a large set of biological data and was first implemented in NEURON (Figure 6) and then translated in NEST. Multicompartmental neuron models, which have been reconstructed and validated beforehand (Masoli *et al.*, 2015; Masoli *et al.*, 2017 P1191 and Masoli *et al.*, 2022, P3875), were used to generate network connectivity and then used for detailed circuit simulations. These were validated against a wealth of experimental data to yield a new ground truth of the functional organisation of the cerebellar network. The network was subsequently transformed in NEST, using EGLIF point neuron models maintaining the salient non-linear neuronal dynamics (Geminiani *et al.*, 2019, P2007 and Geminiani *et al.*, 2018, P1580). The network is now being morphed into the equivalent human version (Figure 7).

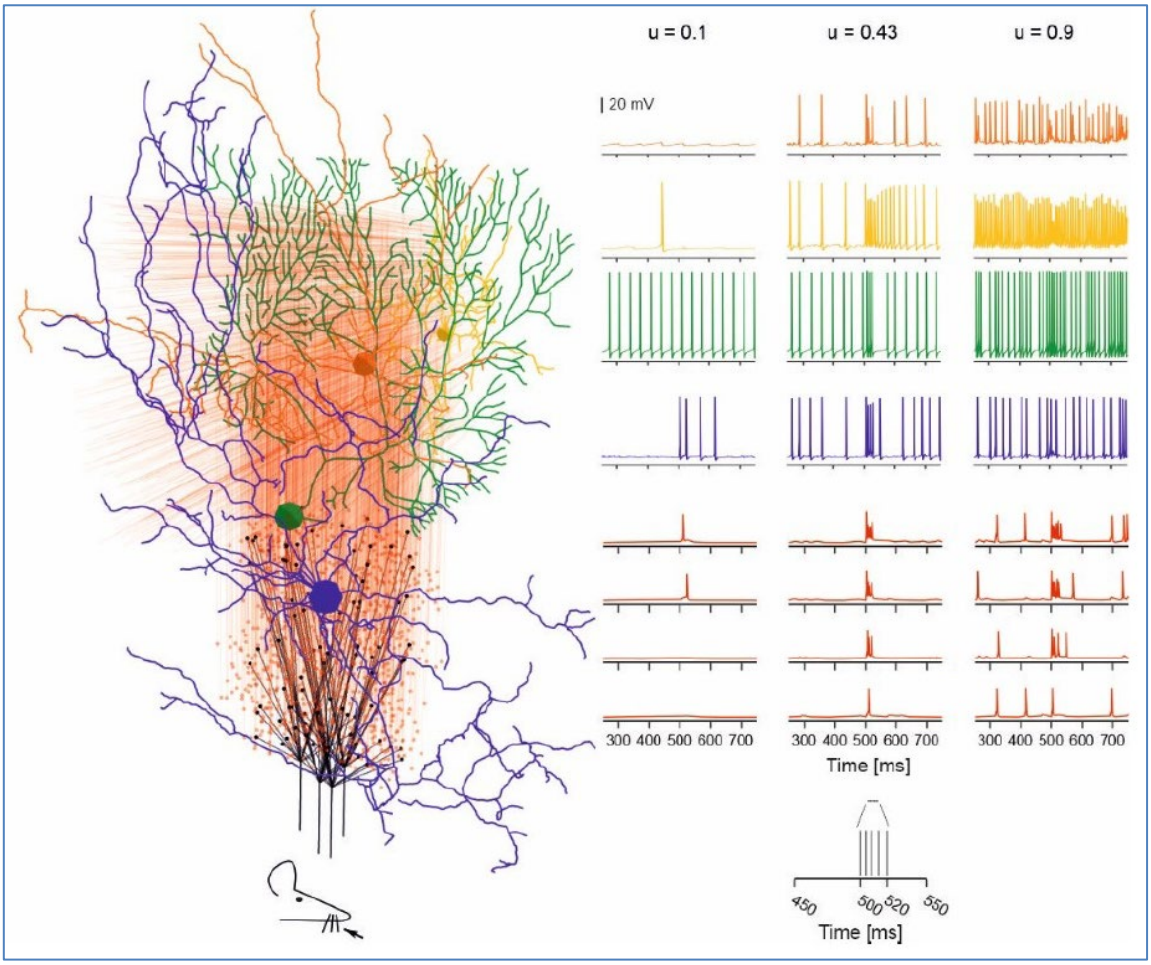

Figure 6: Cerebellar network reconstruction using the BSB

[2] https://ebrains.eu/service/brain-scaffold-builder

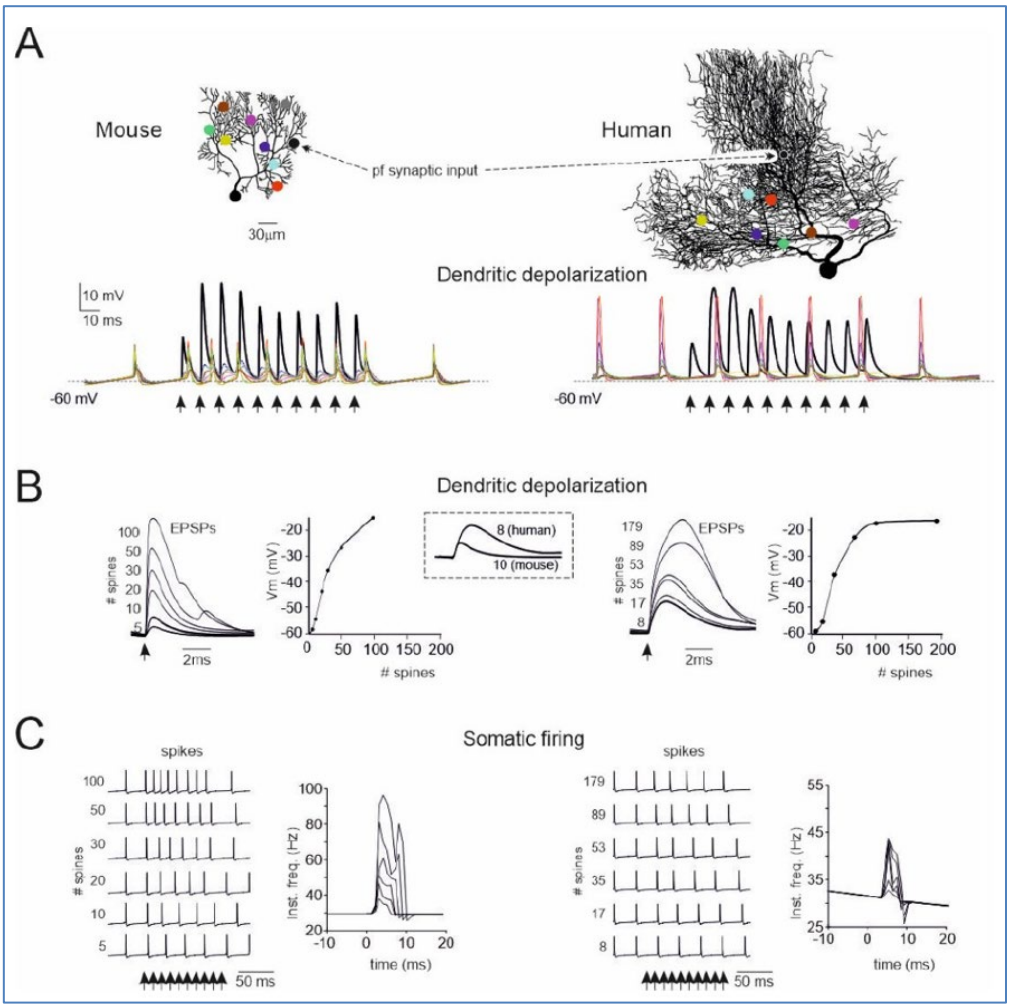

Figure 7: Model simulations of a human Purkinje cell of the cerebellum compared to a mouse PC

A: morphological reconstruction and dendritic membrane potential during simulation of repetitive neurotransmission. B: dendritic EPSPs with different parallel fibre inputs. C: Spike discharge changes in the soma during synaptic activation.

2.2 Mean-field models

2.2.1 Mean-field models of cerebral cortex

Partner CNRS has worked on developing mean-field models of the cerebral cortex, starting with AdEx networks of RS and FS cells (Zerlaut *et al.*, 2018, P1019), then including adaptation (di Volo *et al.*, 2019, P1864) mean-field models, developed for Hodgkin-Huxley models of RS and FS cells (Carlu *et al.* 2020, P2369) and, more recently, heterogeneous mean-field models of RS and FS cells (Di Volo and Destexhe, 2021, P2920). In each case, the mean-field model was validated against the spiking network, for both spontaneous activity and response to external input. The AdEx mean-field model with adaptation was remarkably precise in capturing the network response to stimuli and was chosen as the model to be implemented in EBRAINS (Goldman *et al.*, 2022, P3023). It has been the basis of TVB models for mouse, macaque and human in HBP SGA3 Showcase 3. The behaviour of the cortical mean-field model is described below. Figure 8 shows the typical fitting of RS and FS cell types to the transfer function, which is at the heart of the mean-field formalism. Figure 9 shows the validation of the mean-field model by comparing a spiking network to the mean-field, in the case of a network responding to external inputs.

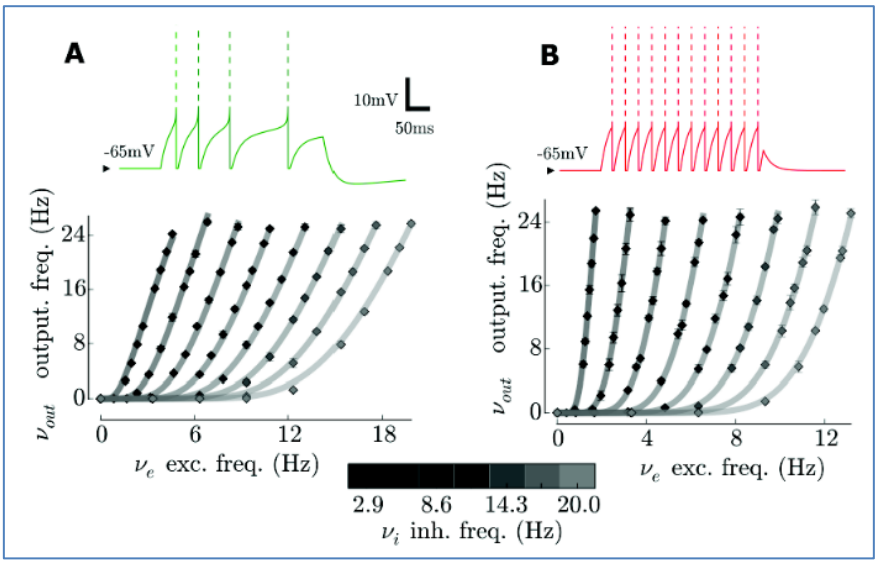

Figure 8: Fitting of the transfer function to calculate the cortical mean-field model

A: RS cells (excitatory). B: FS cells (inhibitory).

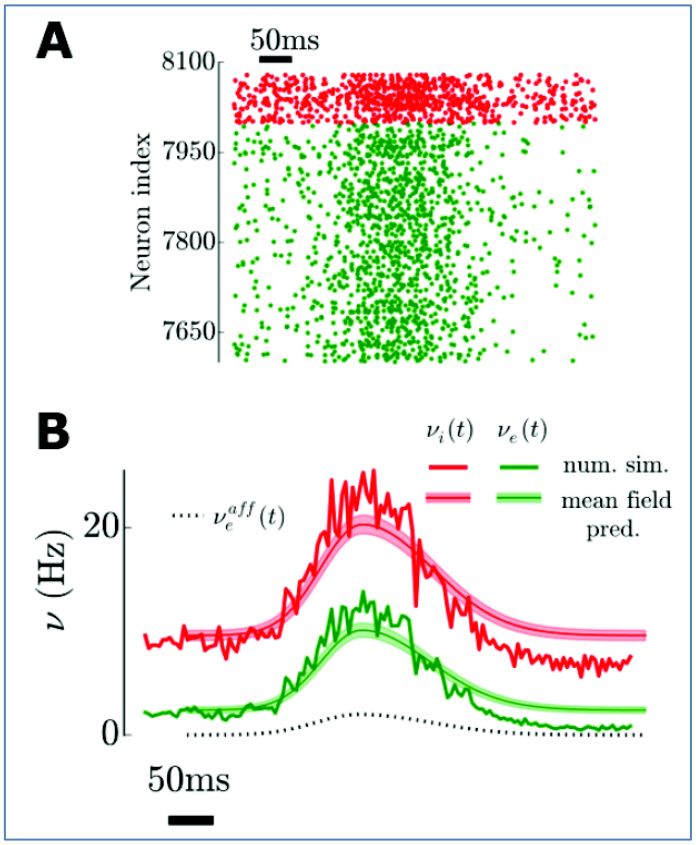

Figure 9: Validation of the mean-field model

A: Raster of the spiking activity of RS (green) and FS (red) cells during the presentation of an external stimulus (Gaussian distributed excitatory synapses). B: Mean activity of each population in the network (noisy curves), compared with the mean-field prediction (continuous curves).

This mean-field model has been implemented in TVB in EBRAINS (Goldman *et al.*, 2022, P3032). It is now available in EBRAINS, for the mouse brain, the monkey brain and the human brain. See https://wiki.ebrains.eu/bin/view/Collabs/showcase-3-tvb-brain-states-modelling/Drive

2.2.2 Mean-field models of hippocampus

Partners CNR, UNIPV and CNRS collaborated to design a mean-field model of hippocampal circuits, starting with the CA1 region of hippocampus. The model comprised excitatory and inhibitory neurons

described by the Extended Generalised IF model (EGLIF). The mean-field was constructed and validated by comparing the network model with the mean-field prediction. The model considered a network made by pyramidal cells and interneurons from CA1. In Figure 10, we show the numerical transfer function obtained for each type of neuron, together with the fit for the semi-analytical transfer function used in the mean-field formalism. This mean-field model was implemented in EBRAINS; see: https://wiki.ebrains.eu/bin/view/Collabs/mean-field-hippocampus/.

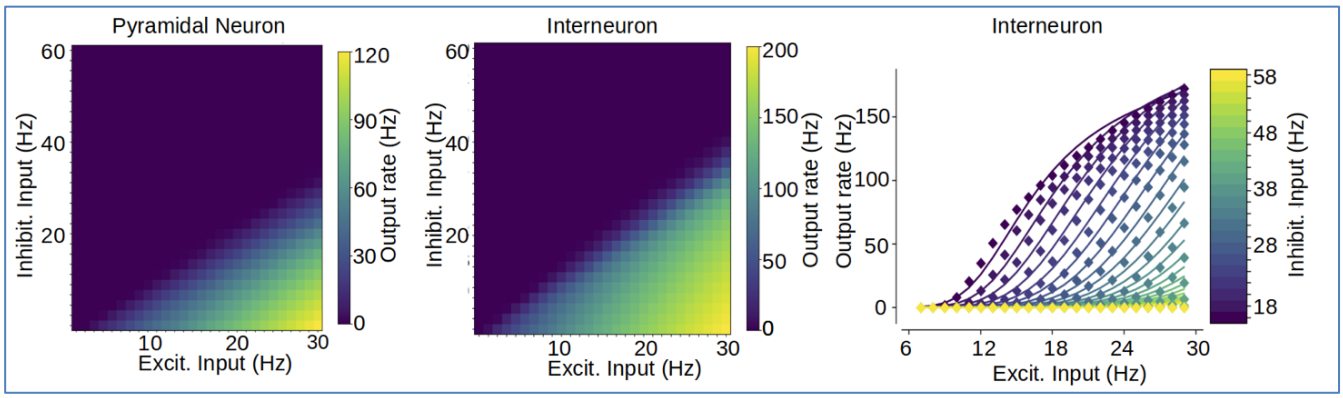

Figure 10: Numerical transfer function (TF) obtained from single cells simulation

Numerical transfer function (TF) obtained from single cells simulations of a representative pyramidal cell (left) and an interneuron (middle) in the CA1 region of the hippocampus. Right: Fitting of the semi-analytical TF for the interneuron.

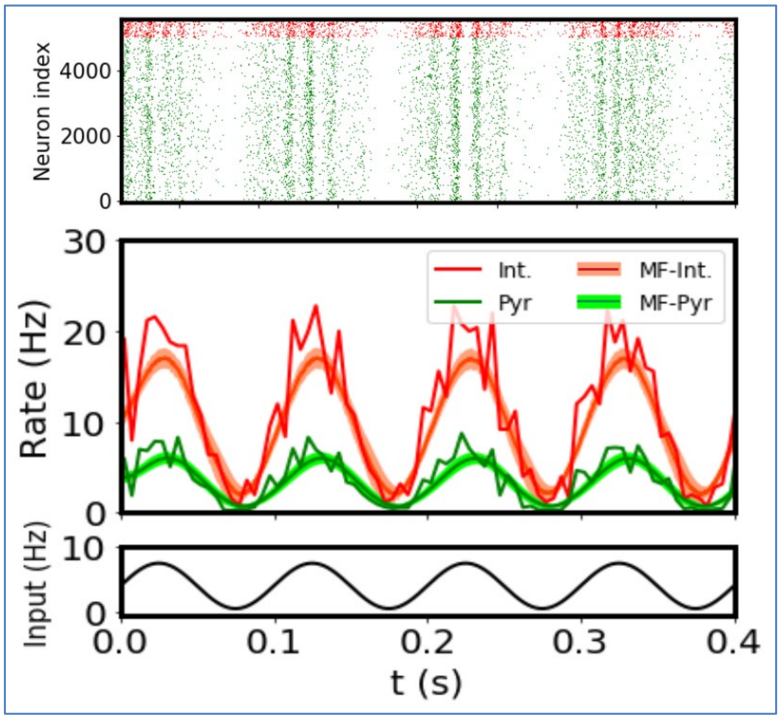

Figure 11: Comparison between the mean-field model and the spiking-network simulations.

Top panel: raster plot of the network for an oscillatory input in the theta band (10Hz). Middle panel: mean firing rate obtained from the network for the Pyramidal and Interneuron cells together with the Mean field model calculations. Bottom panel: external input.

2.2.3 Mean-field models of basal ganglia

Partner KI and CNRS collaborated to design mean-field models of the basal ganglia. The model comprised three different types of striatal cells: fast-spiking interneurons (FS), plus direct and indirect pathway projection neurons (dSPN and iSPN). Each cell type was described by a corresponding Adaptive Exponential Integrate and Fire (AdEx) model. In the network, SPN cells are interconnected, while FS project to SPNs and receive input from other FS cells. This mean-field

model was implemented in EBRAINS, see https://wiki.ebrains.eu/bin/view/Collabs/mean-field-basal-ganglia. In Figure 12, we show the fit of the transfer function for each type of cell in network.

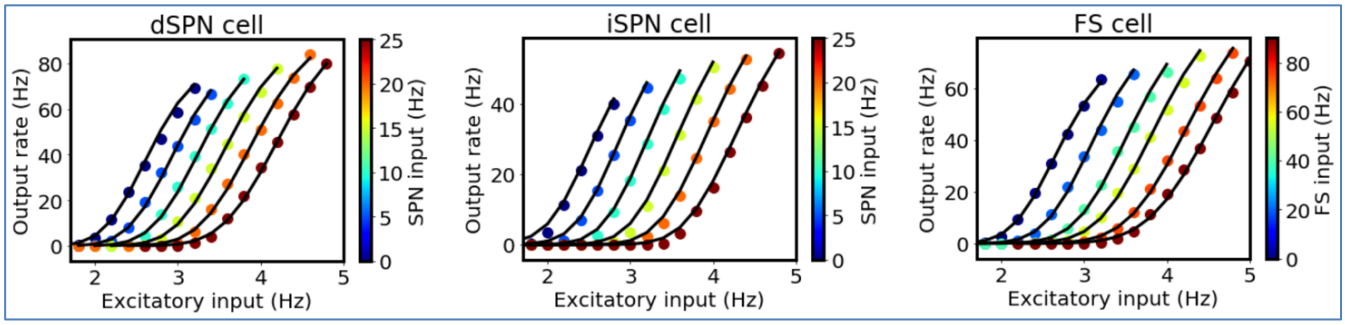

Figure 12: Transfer functions of basal ganglia neurons

Fit of the transfer function for direct projection neurons (dSPN), indirect projection neurons (iSPN) and fast-spiking interneurons (FS) of the basal ganglia (BG).

To validate the mean-field model, in Figure 13 we show the results of network simulations, together with the mean-field predictions. The figure shows the response of the network and the mean-field to an external input.

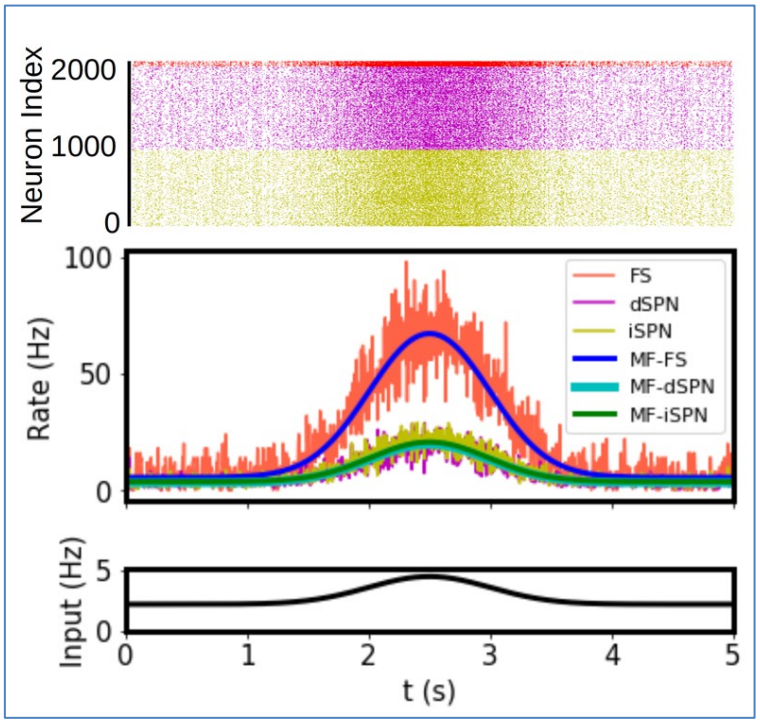

Figure 13: Comparison between spiking network simulations and the mean-field model (MF)

Top: raster plot of the three neuronal populations in the BG (FS in red, dSPN in magenta and iSPN in yellow) during the application of an external input. Middle: mean firing rate and the corresponding mean-field calculation for each population. Bottom: external input

2.2.4 Mean-field models of cerebellum

Partners UNIPV and CNRS collaborated recently to obtain a mean-field model of cerebellum, comprising the different cell types (Purkinje cells, Golgi cells, granule cells, etc). The model was validated against the spiking network (see Section 2.1.4) for responses to different types of stimuli, including oscillatory responses (Lorenzi *et al.*, 2022, P3874).

Figure 14 shows the numerical template of the transfer functions to underline the inter-population differences in working frequencies that are captured by population-specific TFs and, as a consequence, by the MF. Regarding the correspondence between SNN and MF (Figure 15), we show the MF prediction (line) over the SNN results (histogram). We also added a boxplot for Purkinje cells'

activity that are the cerebellar MF output (in practice, the signal that would be input for other cerebellar modules and/or region-specific MFs) to show quantitatively that MF prediction is within SNN output. The protocols we used are realistic patterns simulating sensory stimulus and/or cortical-like patterns. This mean-field model was implemented in EBRAINS; see https://wiki.ebrains.eu/bin/view/Collabs/mean-field-cerebellar/.

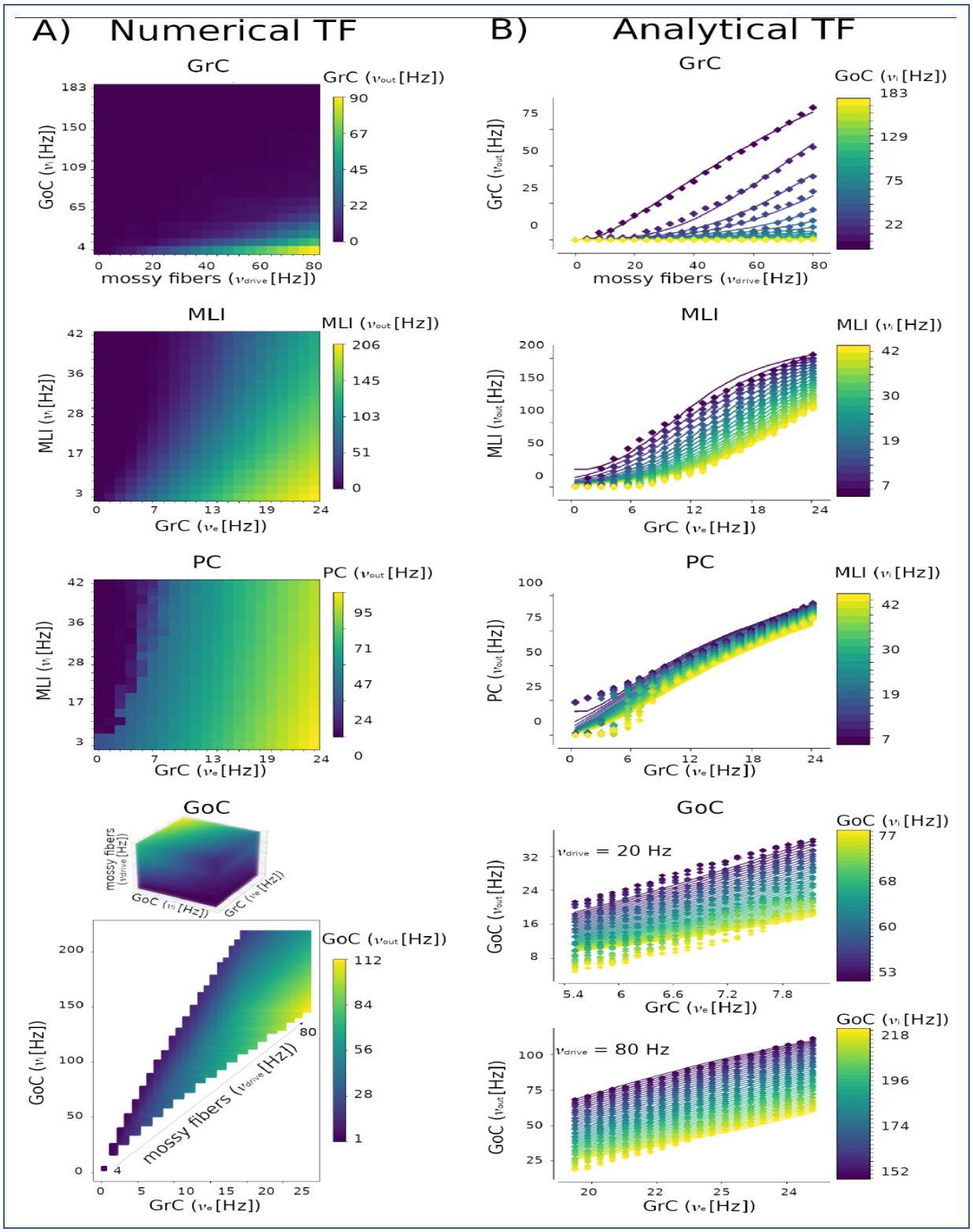

Figure 14: Population-specific Transfer Functions (TFs)

Population-specific Transfer Functions (TFs) reflect differences amongst the populations. A: The numerical templates are extracted from Spiking Neural Network. 2D numerical TF is showed for GrC, MLI and PC, with inputs from 2 presynaptic populations. 3D numerical TF is reported for GoC, receiving input from 3 presynaptic sources: mossy fibres, GrC and GoC. B: Numerical TFs are used to fit the analytical TFs (vout). Excitatory inputs are reported on the x axis, inhibitory ones are colour-coded.

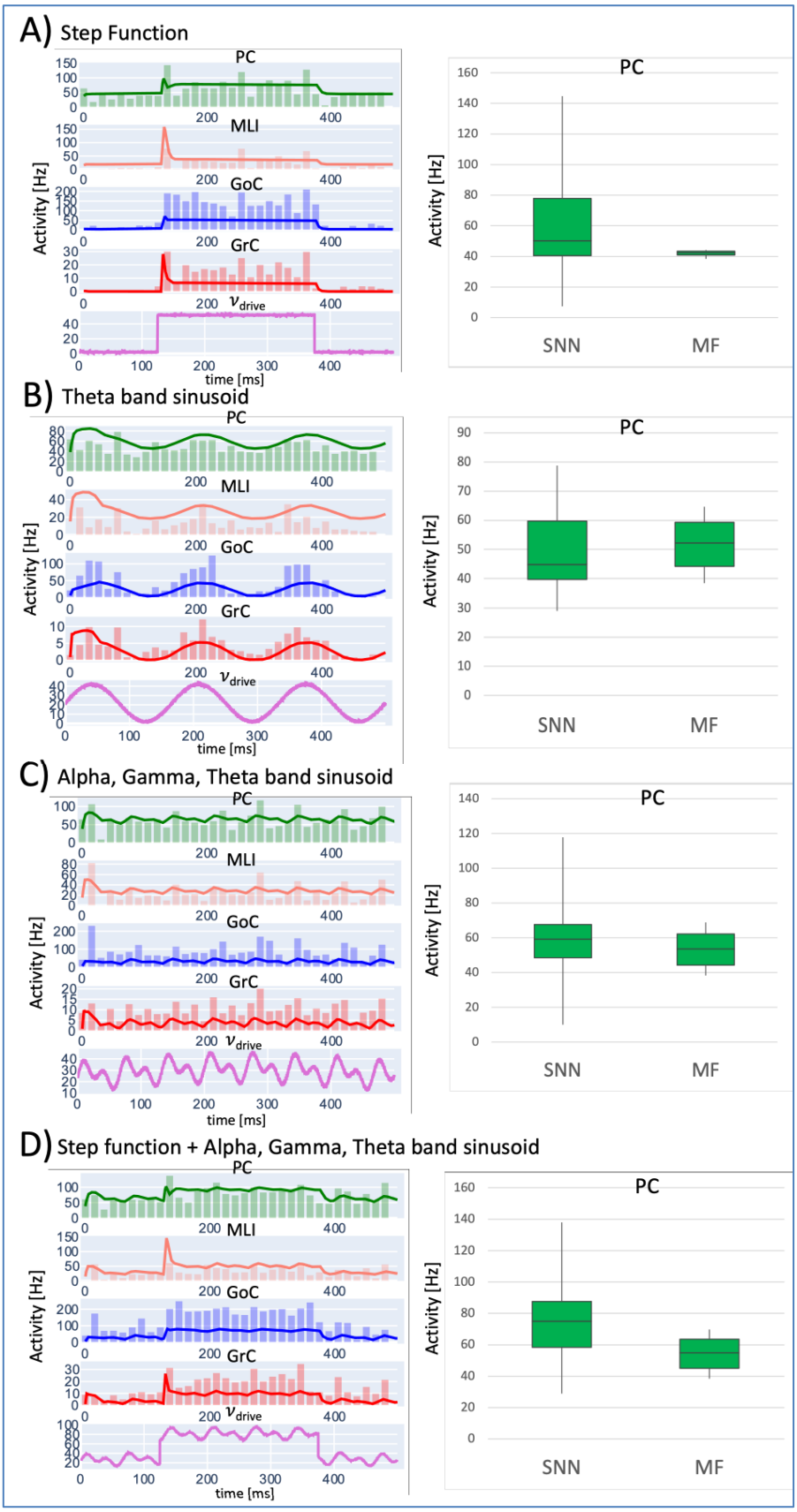

Figure 15: Comparison of Spiking Neural Network and mean-field activity in cerebellar cortical populations

Additional information on Figure 15 above: Comparison of Spiking Neural Network (SNN) and mean-field (MF) activity in cerebellar cortical populations (GrC = Granule Cells, GoC = Golgi Cells, MLI = Molecular Layer Interneurons, PC = Purkinje Cells), in response to different cortical-like driving input patterns (νdrive). The trace of MF activity is overlaid on the spiking activity (Peristimulus Time Histogram, time bins of 15ms). In all cases (A, B, C and D), MF activity is within physiological ranges. Boxplots of PC-simulated activity with SNN and MF show that the MF is able to respond to the different stimulation patterns within the same frequency ranges of SNN.

2.3 Integration in the WP1 reference framework

The multilevel EBRAINS Human Brain Atlas[3] establishes a common reference space where data and models can be represented and spatially anchored. It builds on the Julich-Brain cytoarchitectonic maps, which provide a basis for microstructural reference parcellation. The Atlas facilitates access to spatially resolved data features, including receptor densities, cell distributions, multiple levels of connectivity, physiological recordings and functional imaging.

This rich, spatially organised data can be used to inform and validate models integrated in the same reference space. For this to be practically realisable, the datasets are made interoperable with the modelling services (e.g. The Virtual Brain) through programmatic interfaces (siibra-python[4]) which provide convenient and structured access to the data of the multilevel Human Brain Atlas.

For the mean field models, the integration in the brain reference framework is realised by means of an adapter developed in WP1 for The Virtual Brain. In particular, this adapter was employed to retrieve subject-specific structural connectivities and fMRI data from a cohort dataset to develop a novel causal inference framework in the context of healthy brain ageing (Lavanga *et al.*, 2022, P3860; HBP SGA3 Showcase 1). Furthermore, the AdEx mean field model was integrated in TVB, and makes use of the receptor density maps from the EBRAINS Human Brain Atlas, as described in more detail in the next section.

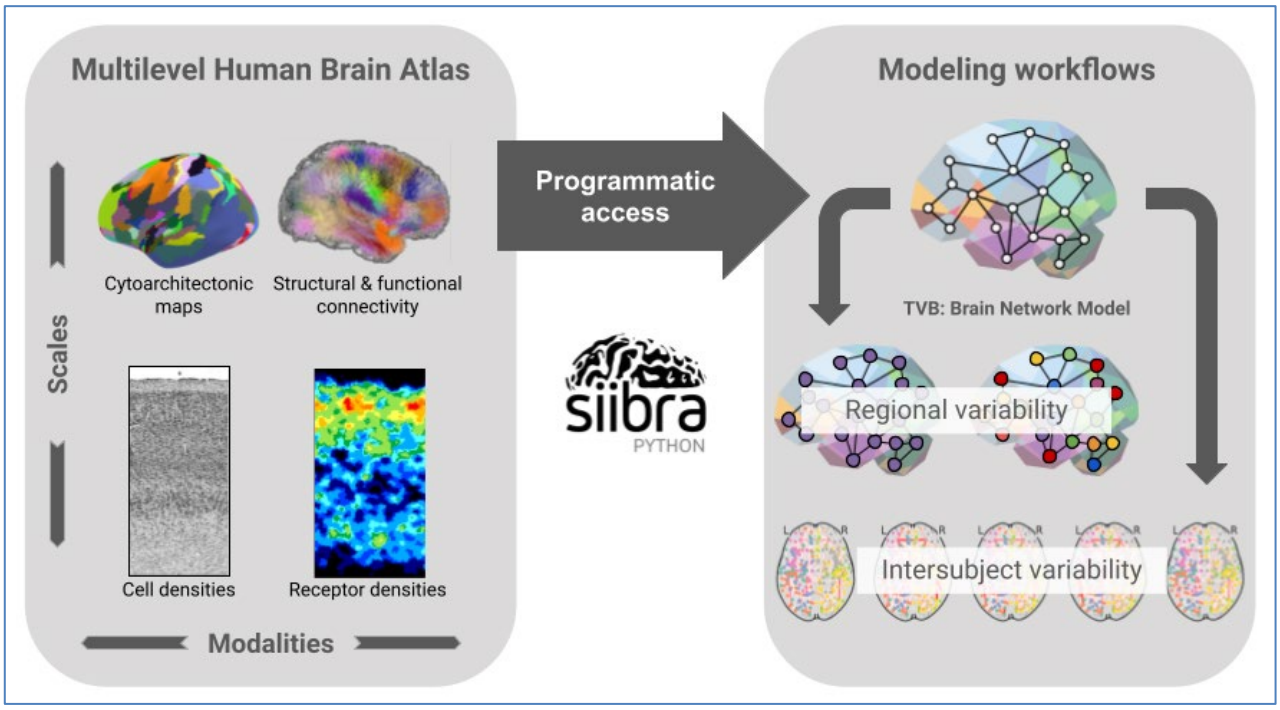

Figure 16: Integration of the modelling workflows in the human atlas reference framework.

Additional information on Figure 16 above: The multilevel Human Brain Atlas (left) provides structural and functional datasets anchored in a common space through a programmatic interface with siibra-python (middle) to inform model building and validation workflows for assessing both variability across individual and brain regions (right).

2.4 Integration with receptor maps

Partner UPF collaborated with Partner CNRS in order to account for regional neuroreceptor densities in two mean-field models: the Montbrió-Pazó-Roxin (MPR) (Montbrió *et al.*, 2015) and the Mean-field AdEx models (Carlu *et al.*, 2020, P2369). In recent years, it has become evident that cortical regions differ in the relative numbers of receptor densities for a variety of neurotransmitters. This

[3] https://ebrains.eu/service/human-brain-atlas
[4] https://github.com/FZJ-INM1-BDA/siibra-python

heterogeneity affects the local behaviour of individual cortical areas and reveals that brain regions will be differently affected by, for example, pharmacological intervention.

The MPR is a model of one population of all-to-all coupled, quadratic integrate-and-fire neurons that consist of two equations, one representing the average membrane potential of the population and the other representing their mean firing rate. We extended the model in order to create a network of brain areas, by modelling each region as a pair of coupled excitatory and inhibitory populations. We included additional equations to couple across populations via synaptic gating variables and added feedback inhibitory control. Finally, modulation of GABAa neuroreceptors for each brain region was included as a fast synaptic variable. The model has been implemented in the TVB simulation engine.

We have adapted the model to simulate a cortical network of mean-field AdEx populations (see Section 2.2.1); Goldman *et al.*, 2022, P3023) developed in TVB for human connectivity (HBP SGA3 Showcase 3) and included a capability for regional modulation of neuroreceptors, especially for GABAa and NMDA. Therefore, we included fast (for GABAa) and slow (for NMDA) synaptic currents for the original equations, with saturation constants proportional to the receptor density observed from empirical data.

Both models are currently being employed in HBP SGA3 Showcase 1 to simulate the effects of Propofol and Ketamine anaesthetics which block GABAa and NMDA neuroreceptors, respectively. Empirical maps of these neuroreceptor densities (Hansen *et al.*, 2022) were provided by HBP partners in Task T1.1 and were made available for testing and validation of the workflows, via the Siibra interface (https://siibra-python.readthedocs.io/en/latest/).

Finally, to continue bridging from the receptor level to the cellular/microcircuit level, Partner KTH has improved autonomised pipelines for optimising models for AMPA/NMDA synapses with short-term plasticity (Carannante *et al.*, 2022, P3872). These model components can then be integrated into microcircuit models. Furthermore, KTH has, together with several other HBP partners, demonstrated how molecular level modelling approaches can inform systems biology models, such as receptor-induced signalling (Keulen *et al.*, 2023, P3700). We have also highlighted and reviewed the use of FAIR modelling workflows for bridging between molecules, synapses and microcircuits (Eriksson *et al.*, 2022, P3699).

3. Looking Forward

The models described in this Deliverable show the multi-scale, multi-region investigation done in WP1 Tasks T1.5 and T1.6. The microcircuit models are conceived first in this bottom-up approach, and mean-field techniques are employed to yield population models for each brain region. These mean-field models are then integrated in large-scale simulations using TVB, allowing us to reach the whole-brain level. This work thus spans multiple scales, from single cells to the whole brain.

The essential perspective is to integrate all these models in TVB into a single whole-brain simulation with interacting brain regions. To do this, we must first investigate the “mesoscale” level (millimetres) and reconstruct large-scale models of entire brain regions. For example, modelling primary visual cortex (V1) can be done using a large number of mean-field nodes, connected together using the V1 connectivity data. This was done for simple activity patterns such as propagating waves (Zerlaut *et al.*, 2018). We would like to follow the same approach to simulate the entire hippocampus, the entire cerebellum and the entire basal ganglia. Note that mean-field models of the thalamus are in preparation (not shown here) and will be essential to connect the different brain structures.

The final step will be to assemble the brain region models into a whole-brain simulation, the precision of which will depend on the connectome data available. This is where EBRAINS can play a particularly useful role, by allowing us to use anatomical data (Human Brain Atlas), with the simulation capacities of TVB, possibly with the help of large-scale computing resources (HPC). All these components are present in EBRAINS, so we anticipate that this will enable the building of such multi-scale models.

4. References

P2369: Carlu, M., Chehab, O., Dalla Porta, L., Depannemaecker, D., Herice, C., Jedynak, M., Koksal Ersoz, E., Muratore, P., Souihel, S., Capone, C., Zerlaut, Y., Destexhe, A., di Volo, M. A mean-field approach to the dynamics of networks of complex neurons, from nonlinear Integrate-and-Fire to Hodgkin-Huxley models. J. Neurophysiol. 123: 1042-1051, 2020.

P3872 : Carannante Ilaria, Johansson Yvonne, Silberberg Gilad, Hellgren Kotaleski Jeanette (2022) Data-Driven Model of Postsynaptic Currents Mediated by NMDA or AMPA Receptors in Striatal Neurons, Frontiers in Computational Neuroscience 16. DOI=10.3389/fncom.2022.806086.

P3729: Robin De Schepper, Alice Geminiani, Stefano Masoli, Martina Francesca Rizza, Alberto Antonietti, Claudia Casellato, Egidio D'Angelo (2022) Model simulations unveil the structure-function-dynamics relationship of the cerebellar cortical microcircuit. Commun Biol. http://dx.doi.org/10.1038/s42003-022-04213-y.

P1864: Di Volo, M., Romagnoni, A., Capone, C. and Destexhe, A. Biologically realistic mean-field models of conductance-based networks of spiking neurons with adaptation. Neural Computation 31: 653-680, 2019.

P2920: Di Volo and and Destexhe. Optimal responsiveness and information flow in networks of heterogeneous neurons (2021). Sci. Rep. doi: 10.1038/s41598-021-96745-2

E. Monbtrió, D. Pazó and A. Roxin (2015) Macroscopic Description for Networks of Spiking Neurons. Phys. Rev. X 5, 021028. DOI: http://dx.doi.org/10.1103/PhysRevX.5.021028.

P3699: Eriksson O, Bhalla US, Blackwell KT, Crook SM, Keller D, Kramer A, Linne M-J, Saudargienė A, Wade RC and Hellgren Kotaleski J. (2022) Combining hypothesis- and data-driven neuroscience modeling in FAIR workflows *eLife* 11:e69013; https://doi.org/10.7554/eLife.69013

P2674: Frost Nylén J, Carannante I, Grillner S, Hellgren Kotaleski J. Reciprocal interaction between striatal cholinergic and low-threshold spiking interneurons - A computational study. Eur J Neurosci. 2021 Apr;53(7):2135-2148. doi: 10.1111/ejn.14854. Epub 2020 Jun 26.PMID: 32511809

Gandolfi D, Mapelli J, Triebkorn P, Solinas S, D'Angelo E, Jirsa V, Migliore M, Full-scale scaffold model of the human hippocampus CA1 area, Nature Computational Science, in press, 2023.

P2007: Geminiani, A., Casellato, C., D'Angelo, E., and Pedrocchi, A. (2019). Complex Electroresponsive Dynamics in Olivocerebellar Neurons Represented With Extended-Generalized Leaky Integrate and Fire Models. Front. Comput. Neurosci. 13, 1–12. doi:10.3389/fncom.2019.00035.

P1580: Geminiani, A., Casellato, C., Locatelli, F., Prestori, F., Pedrocchi, A., and D'Angelo, E. (2018). Complex dynamics in simplified neuronal models: Reproducing golgi cell electroresponsiveness. Front. Neuroinform. 12, 1–19. doi:10.3389/fninf.2018.00088

P3023: Goldman, J.S., Kusch, L., Aquilue, D., Yalcinkaya, B.H., Depannemaecker, D., Ancourt, K., Nghiem, T-A., Jirsa, V. and Destexhe, A. A comprehensive neural simulation of slow-wave sleep and highly responsive wakefulness dynamics. Frontiers in Computational Neuroscience 16: 1058957, 2022.

P2489: Hjorth JJJ, Kozlov A, Carannante I, Frost Nylén J, Lindroos R, Johansson Y, Tokarska A, Dorst MC, Suryanarayana SM, Silberberg G, Hellgren Kotaleski J, Grillner S. The microcircuits of striatum in silico. Proc Natl Acad Sci U S A. 2020 Apr 28;117(17):9554-9565

P3873 : Hunt et al., (2022). Strong and reliable synaptic communication between pyramidal neurons in adult human cerebral cortex, Cerebral Cortex. https://doi.org/10.1093/cercor/bhac246.

J.Y. Hansen, G. Shafiei, R.D. Markello, et al. (2022) Mapping neurotransmitter systems to the structural and functional organization of the human neocortex. Nat. Neurosci. 25, 1569 – 1581. DOI: https://doi.org/10.1038/s41593-022-01186-3.

P3860: Lavanga, M., Stumme, J., Yalcinkaya, B. H., Fousek, J., Jockwitz, C., Sheheitli, H., Bittner, N., Hashemi, M., Petkoski, S., Caspers, S., & Jirsa, V. (2022). The virtual aging brain: a model-driven explanation for cognitive decline in older subjects. In *bioRxiv* (p. 2022.02.17.480902). https://doi.org/10.1101/2022.02.17.480902.

P3874 : Lorenzi, R.M., Geminiani, A., Zerlaut, Y., Destexhe, A., Gandini Wheeler-Kingshott, C.A.M., Palesi, F., Casellato, C., and D'Angelo E. A multi-layer mean-field model for the cerebellar cortex: design, validation, and prediction. bioRxiv (2022) https://www.biorxiv.org/content/10.1101/2022.11.24.517708v1

Masoli, S., Solinas, S. and D'Angelo, E. Action potential processing in a detailed Purkinje cell model reveals a critical role for axonal compartmentalization (2015). https://doi.org/10.3389/fncel.2015.00047.

P1191: Masoli S, Rizza MF, Sgritta M, Van Geit W, Schürmann F, D'Angelo E. Single Neuron Optimization as a Basis for Accurate Biophysical Modeling: The Case of Cerebellar Granule Cells. Front. Cell. Neurosci, 15 March 2017. http://dx.doi.org/10.3389/fncel.2017.00071.

P3875 : Masoli, S., Rizza, M. F., Tognolina, M., Prestori, F., and D'Angelo E (2022) Computational models of neurotransmission at cerebellar synapses unveil the impact on network computation. https://doi.org/10.3389%2Ffncom.2022.1006989.

Rizza MF, Locatelli F, Masoli S, Sánchez-Ponce D, Muñoz A, Prestori F, D'Angelo E. Stellate cell computational modeling predicts signal filtering in the molecular layer circuit of cerebellum. Sci Rep. 2021 Feb 16;11(1):3873. doi: 10.1038/s41598-021-83209-w. PMID: 33594118; PMCID: PMC7886897.

Siri C. Keulen, Juliette Martin, Francesco Colizzi, Elisa Frezza, Daniel Trpevski, Nuria Cirauqui Diaz, Pietro Vidossich, Ursula Rothlisberger, Jeanette Hellgren Kotaleski, Rebecca C. Wade, Paolo Carloni (2023) Multiscale molecular simulations to investigate adenylyl cyclase-based signaling in the brain. WIREs Computational Molecular Science: https://doi.org/10.1002/wcms.1623.

P1019: Zerlaut, Y., Chemla, S., Chavane, F. and Destexhe, A. Modeling mesoscopic cortical dynamics using a mean-field model of conductance-based networks of adaptive exponential integrate-and-fire neurons. J. Computational Neurosci. 44: 45-61, 2018. https://doi.org/10.1007/s10827-017-0668-2.